The Journal's name will be set by the publisher
DOI: will be set by the publisher

Imaging Demonstration of a Glass Gas Electron Multiplier with Electronic Charge Readout

Yuki Mitsuya[1,a], Patrik Thuiner[2,4], Eraldo Oliveri[4], Filippo Resnati[4], Miranda van Stenis[4], Takeshi Fujiwara[3], Hiroyuki Takahashi[1], and Leszek Ropelewski[4]

[1] *The University of Tokyo*
[2] *Vienna University of Technology*
[3] *National Institute of Advanced Industrial Science and Technology*
[4] *European Organization for Nuclear Research (CERN)*

Abstract. We have developed a Glass Gas Electron Multiplier (Glass GEM, G-GEM), which is composed of two copper electrodes separated by a photosensitive etchable glass substrate having holes arranged in a hexagonal pattern. In this paper, we report the result of imaging using a G-GEM combined with a 2D electronic charge readout. We used a crystallized photosensitive etchable glass as the G-GEM substrate. A precise X-ray image of a small mammal was successfully obtained with position resolutions of approximately 110 to 140 μm in RMS.

1 Introduction

The gas electron multiplier is one of the most commonly used Micro Pattern Gas Detectors [1]. It has a large-area imaging capability with high position resolution because of its numerous microholes. Its high degree of freedom – detector design – is also attractive; since it only multiplies electrons, it can be combined with a variety of readout systems, or other types of MPGDs as their preamplifier.

Recently, we developed a new type of MPGD, Glass Gas Electron Multiplier (G-GEM) [2]. The G-GEM's substrate is composed of the photosensitive etchable glass, PEG3 (HOYA Corporation, Japan). Holes of the G-GEM are uniformly fabricated using a photolithography technique over the entire sensitive area. The G-GEM is appropriate for sealed-type detectors since it is free of outgassing. The G-GEM has the sufficiently thick glass substrate to support itself over the sensitive area. However, if we use the thick substrate, the charge-up of avalanche electrons on the hole surface becomes serious because the large part of the insulator is exposed to the operational gas. This problem is resolved by using the low volume resistivity glass for the substrate. The resistivity of PEG3 (8.5×10^{12} Ω·cm) is sufficiently low to reduce charge-up.

The large-area imaging device with a gas detector will be attractive for various fields: imaging of heavy charged particles, which normally cause severe radiation damages to solid state detectors; large-area neutron imaging combined with a solid state converter like ^{10}B; and imaging of low energy X-rays (several keV), which cannot be observed clearly with solid state detectors because of the low signal levels against them. In addition, if the detector does not outgas and can be operated stably under sealed condition, all the gas circulating or purifying systems can be removed; It will greatly improve the portability of the imaging device. The portability is necessary for the on-site use of the detector: for example, at the scene of radiotherapy in the hospitals. The sealed-type detector can be also used for gaseous photomultiplier applications. The sealed-type detector is also compatible with the rare and expensive gases like Xenon, which have higher detection efficiency against X-rays. Realizing this kind of portable gas-sealed type imaging device is made possible by G-GEM's non-outgassing property. In addition, the high gain capability of G-GEM with single stage and self-supporting structure, make an attractive imaging device.

In this study, we demonstrate the imaging capability of G-GEM using a two-dimensional electronic charge readout system. We report on the results, and discuss the position resolution obtained with the setup.

2 Experimental setup

In this experiment, we used a single G-GEM made of crystallized glass, which is a crystallized version of PEG3, called PEG3C (HOYA Corporation, Japan) for measurements. PEG3C has higher resistivity (4.5×10^{14} Ω·cm) than that of PEG3 (8.5×10^{12} Ω·cm). However, the mechanical strength of PEG3C is improved compared with PEG3 glass, which means that the PEG3C can be used with a wider variety of designs including those with thinner structure [3]. The sensitive area of the G-GEM is 100 $\times$ 100 mm^2. The thickness, hole pitch, and hole diameter are 680 μm, 280 μm, and 170 μm respectively.

[a] e-mail: yukimitsuya@sophie.q.t.u-tokyo.ac.jp

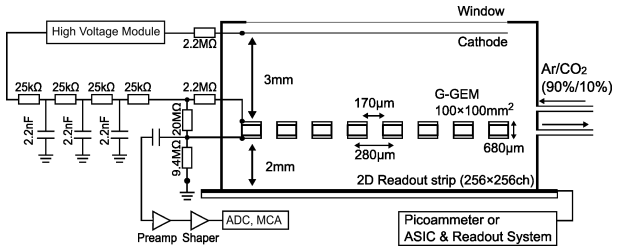

Figure 1. Setup of experiments

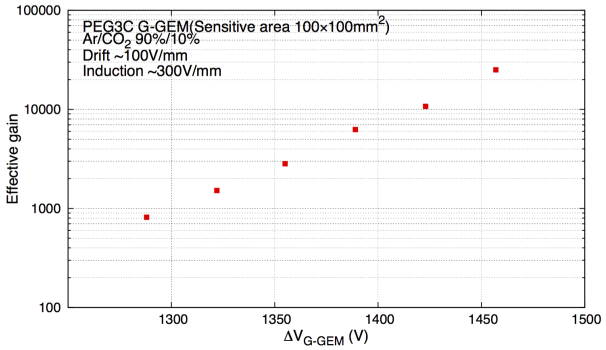

Figure 2. Gain curve of PEG3C G-GEM

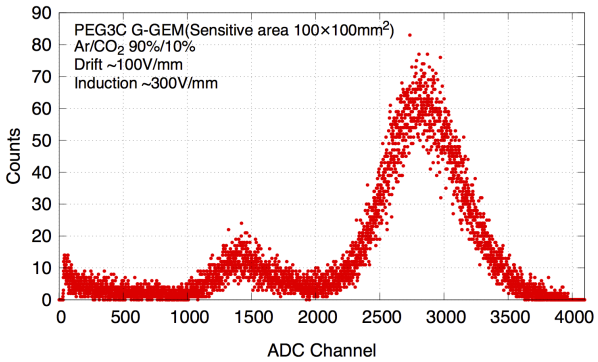

Figure 3. Pulse height spectrum obtained from the bottom of the G-GEM

Figure 1 is the experimental setup. We installed a drift cathode 3 mm above and a readout 2 mm under the G-GEM. The G-GEM was powered with a voltage divider composed of high voltage resistors. The drift field was 1 kV/cm, and the induction field was 3 kV/cm. A charge-sensitive preamplifier was connected to the bottom of G-GEM with an AC coupling capacitor, and the preamplifier output was connected to a shaping amplifier and an MCA for capturing pulse height spectra. The detector was flushed with an Ar/CO_2 90/10 gas mixture at 6 L/h of flow rate.

The 2D readout anode consists of two planes of 256 parallel copper strips, with the upper one (x-axis) arranged perpendicular to and separated from the lower one (y-axis) by Kapton ridges of 50 μm thickness. The strips of both axes have a pitch of 400 μm, with a strip width of 80 μm and 340 μm for the x-axis and y-axis, respectively, to allow equal charge sharing between both planes. For gain calibration, all the strips of the anode were shorted and read out with a Keithley 6487 picoammeter. For gain uniformity measurement and imaging demonstration, we installed four APV25s and a Scalable Readout System (SRS) to read analogue signals from each strip independently [4].

3 Gain and spectrum measurement

Effective gain of PEG3C G-GEM was calibrated with ^{55}Fe source. For gain measurement, a picoammeter was connected to the readout board. Effective gain G_{eff} was calibrated with the following equation.

$$I = n \cdot e \cdot f \cdot G_{eff} \quad (1)$$

Where I is the readout current, e is the elementary charge, f is the interaction rate measured with MCA and also with the scaler, which counted the rate of pulses from the bottom of G-GEM.

The maximum effective gain reached 2.5 $\times$ 10^4 (figure 2). High gain was obtained with a single PEG3C G-GEM. The pulse height spectrum was also measured with the signals from the bottom of G-GEM (figure 3). The energy resolution was 25.7 % at full-width half maximum (FWHM) of the Gaussian-fitted result at the gain of 1.07 $\times$ 10^4. We also observed a polarization effect after powering the G-GEM. It caused approximately 20 % of gain decrease in the timescale of 40 min; therefore, the detector was kept powered on for more than several hours before the imaging demonstration in order to exclude the polarization effect.

4 Gain uniformity

Before imaging, the global gain uniformity was measured for the PEG3C G-GEM. If there are large differences in gains, by point, over the sensitive area, some parts of the sensitive area could not be biased sufficiently for imaging. In this case, signal-to-noise ratios become worse at the parts where the gains are not enough, or signal levels become incompatible with the following electronics.

For uniformity measurement, the gain of G-GEM was set at 2500. First, we measured the total collected charges by ^{55}Fe irradiation over the 100 $\times$ 100 mm^2 sensitive area. We also measured the total hit counts at the same time. Then the charge map and hit count map were binned into 10 $\times$ 10 bins. Finally, the charge map was divided by the hit count map, which provides information equivalent to the gain map. Figure 4 shows the gain map, which was normalized at an arbitrary point.

The edge 36 bins were excluded for a uniformity evaluation because they are normally affected by field distortions. Some strips having abnormally less hit counts in the longitudinal direction of the middle of the sensitive area were also excluded from evaluation due to statistical inconsistency: The reason of less hit counts in this region is considered attributable to strip or channel defects in the ASIC. As a result, the maximum normalized gain became 1.09, and the minimum became 0.87. Good uniformity

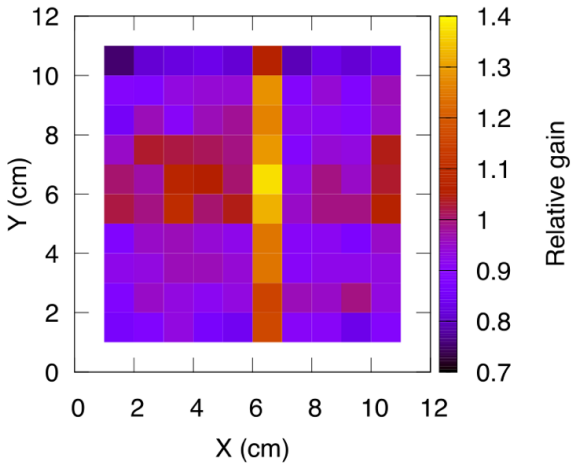

Figure 4. Normalized gain map of 100 × 100 mm^2 sensitive area. The high gain parts for the longitudinal bins in the middle are considered to be due to strip or channel defects.

over the sensitive area was obtained, which proved a sufficient level for the imaging applications.

5 X-ray imaging

We demonstrated imaging of a small mammal (bat) and evaluated the total position resolution. The bat has been used for the imaging demonstration of the standard GEM in the past [5]. We took its X-ray image again with the G-GEM. The bat was placed onto the detector window together with an aluminum block, and Kapton strips of 200 μm width and 1 mm pitch – with the last two being used for position resolution estimation. The ^{55}Fe source was placed approximately 60 cm over the detector to ensure sufficiently parallel beams. The gain was set to approximately 2500. Figure 5 is a photograph of the bat and the Kapton strip before being placed on the detector. Figure 6 and 7 is the imaging result of 100 × 100 mm^2 area with four million hit events in total. The skeletal structure is clearly visible, although a large number of the photons were stopped by the bones because of the low energy source. Additionally, each of the Kapton 200 μm strips can clearly be discriminated. In order to estimate the position resolutions in detail, the edge profiles (arrays of hit count bins) were extracted for both X and Y directions from the edges of aluminum blocks. The edge profiles were then fitted with the Error function as shown below.

$$f(x) = a \cdot erf\left(\frac{x-\mu}{\sqrt{2}\sigma}\right) + c \qquad (2)$$

where x is the position, μ is the expectation of edge position, σ is the standard deviation, a is the scaling factor and c is the offset. Figure 8 and 9 show edge profiles and fitted curves. The position resolutions were σ = 137 μm in the X direction, and 114 μm in the Y direction (RMS). It should be noted that the resolutions were not guaranteed sufficiently due to the rather small data counts for each bin.

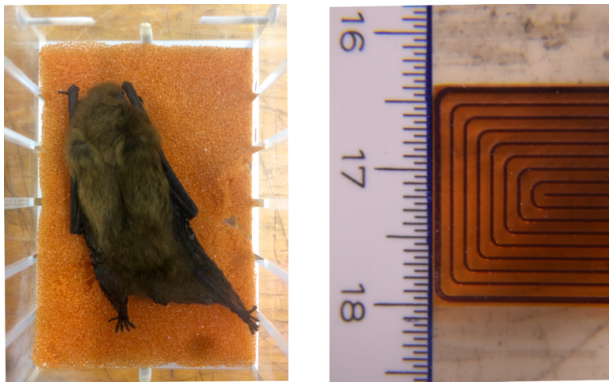

Figure 5. Photographs of the bat and kapton strip

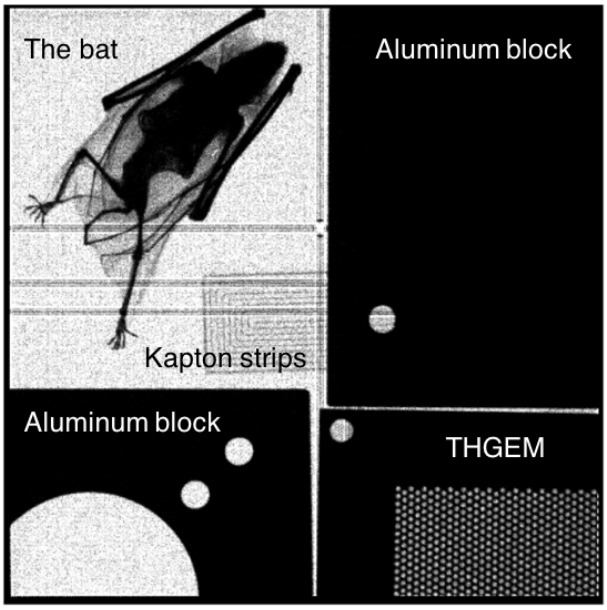

Figure 6. X-ray image of the whole sensitive area

6 Conclusion

In this study, the imaging demonstration of a G-GEM with electronic charge readout was successfully conducted. We used a G-GEM made of crystalized photosensitive etchable glass, PEG3C. The G-GEM showed high gain of 2.5 × 10^4 at maximum with single stage. The global gain uniformity was approximately within ± 10 % over the sensitive area. We obtained a precise X-ray image of a small mammal with the G-GEM combined with the electronic charge readout system and achieved high position resolutions of σ = 137 μm in the X direction and σ = 114 μm in the Y direction (RMS). As these results illustrate, the G-GEM is prospective as an imaging detector, and the future development of a sealed-type imaging device is expected.

References

[1] F. Sauli, Nucl. Instr. and Meth. Phys. Res. A **386**, 531(1997)

[2] H. Takahashi, Y. Mitsuya, T. Fujiwara, et al., Nucl. Instr. and Meth. Phys. Res. A **724**, 1 (2013)
[3] F. Tokanai, et al., Nucl. Instr. and Meth. Phys. Res. A **732** 273 (2013)
[4] S. Martoiu, et al., IEEE NSS-MIC Conference record, N43-5, 2036 (2011)
[5] S. Bachmann, L. Ropelewski, F. Sauli, et al, Nucl. Instr. and Meth. Phys. Res. A, **478** 104 (2002)

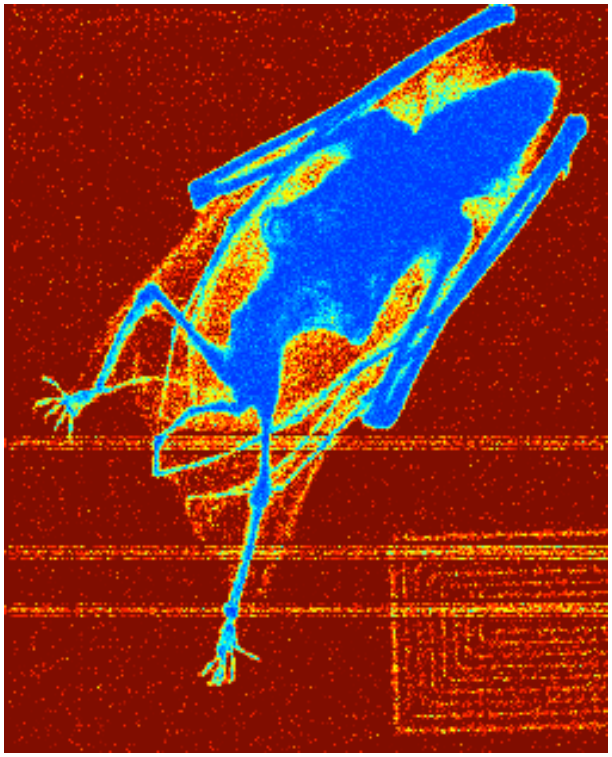

Figure 7. X-ray image of the bat

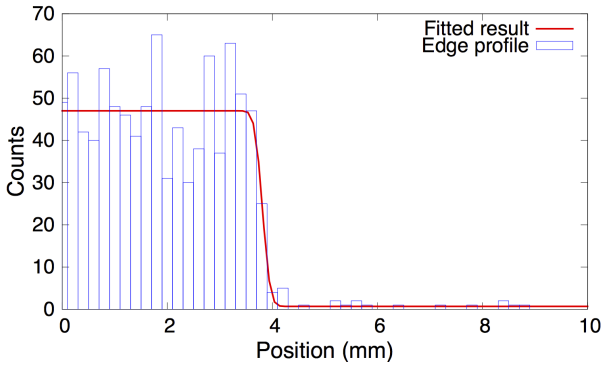

Figure 8. Fitted result of an edge in X direction using the Error function

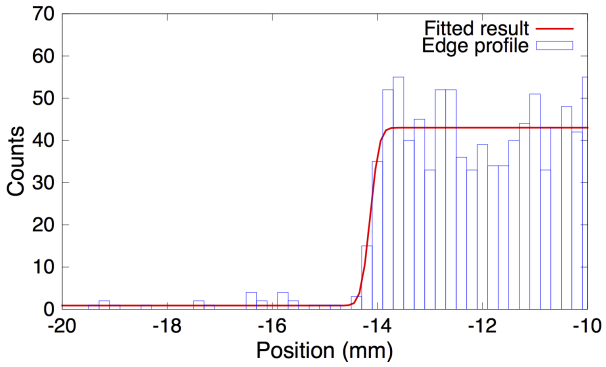

Figure 9. Fitted result of an edge in Y direction using the Error function